Separation Science and Technology
Publication details, including instructions for authors and subscription information:
http://www.informaworld.com/smpp/title~content=t713708471

Environmental Application of Chitosan-Supported Catalysts: Catalytic Hollow Fibers for the Degradation of Phenolic Derivatives

Eric Guibal[a]; Thierry Vincent[a]; Sylvie Spinelli[a]
[a] Ecole des Mines d'Alès, Laboratoire Génie de l'Environnement Industriel, Alès Cedex, France

To cite this Article Guibal, Eric , Vincent, Thierry and Spinelli, Sylvie(2005) 'Environmental Application of Chitosan-Supported Catalysts: Catalytic Hollow Fibers for the Degradation of Phenolic Derivatives', Separation Science and Technology, 40: 1, 633 — 657
To link to this Article: DOI: 10.1081/SS-200042625
URL: http://dx.doi.org/10.1081/SS-200042625

Separation Science and Technology, 40: 633–657, 2005

ISSN 0149-6395 print/1520-5754 online
DOI: 10.1081/SS-200042625

Environmental Application of Chitosan-Supported Catalysts: Catalytic Hollow Fibers for the Degradation of Phenolic Derivatives

Eric Guibal, Thierry Vincent, and Sylvie Spinelli
Ecole des Mines d'Alès, Laboratoire Génie de l'Environnement Industriel, Alès Cedex, France

Abstract: Hollow fibers made of chitosan were prepared and tested for the immobilization of palladium, a catalytic metal widely used for reductive reactions. Hollow chitosan fibers were prepared by extrusion of chitosan into a coagulating solution followed by a final conditioning step to increase the stability of chitosan in acidic solutions. The fibers were then contacted with palladium solution at pH 2; the Pd-loaded hollow fiber was finally chemically reduced with zinc powder in contact with sulfuric acid solution (in situ hydrogen production). The catalytic unit was designed as a two-compartment cell separated by the hollow fiber acting as a catalytic membrane. The solution to be treated was flowed through the lumen of the fiber, while the reductive medium was maintained outside the membrane. Two different reducing agents were used. The first was sodium formate, circulating outside the fiber. The alternative hydrogen donor was hydrogen gas maintained at a given pressure in the reductive compartment. The system was tested for the degradation of phenol derivatives. The efficiency of the catalytic process was evaluated in terms of experimental parameters such as the pH of the solution, the concentration (or pressure) of the reducing agent, the concentration of the phenol derivative, and the residence time in the fiber. The system proved to be of interest for the degradation of phenol derivatives under mild conditions (pressure, temperature, etc.).

The authors thank ANVAR (Agence Nationale de Valorisation de la Recherche, France) for their financial support in the development of chitosan-based catalysts.

Address correspondence to Eric Guibal, Ecole des Mines d'Alès, Laboratoire Génie de l'Environnement Industriel, 6 avenue de Clavières, F-30319 Alès Cedex, France. Fax: +33 (0)4 66 78 27 01; E-mail: Eric.Guibal@ema.fr

INTRODUCTION

The increasingly drastic regulations imposed on the discharge of wastewater into the environment have led to great interest in the development of new treatment processes. Recently, a good deal of attention has been paid to phenol derivatives, most of them being classified in the U.S. Environmental Protection Agency (EPA) list. Conventional treatments consist of coagulation/flocculation processes or adsorption (1, 2). Catalytic reactions have been proposed, including photooxidation (3, 4). The need for cost-efficient, environmentally friendly, and low-energy methods for the treatment of effluents containing phenol derivatives has been the motive for the development of catalytic processes (5–7). These reactions may be used not only for the degradation of phenol derivatives (8, 9) but also for the production of chemical intermediates for fine chemical synthesis (10, 11). All these factors make the study of catalytic transformation of phenol substitutes a promising research area.

Many of the catalytic hydrogenation processes used for nitrophenol and chlorophenol transformation involve precious metals such as platinum and palladium. Taking into account the cost and strategic importance of these metals, as well as the necessity of obtaining them in their reduced oxidation state (metal), supported catalysis has been preferred for optimizing the catalytic hydrogenation of phenol derivatives. In most cases, precious metals are immobilized on activated carbon (12, 13), silica (14), or alumina (15). Recently, however, much interest has been paid to the use of polymeric materials for the development of supported catalysis involving precious metals. Polymeric supports may offer increased selectivity in the chemical reactions (16, 17). While most of these recent research studies have used synthetic polymers, increasing numbers of papers are being published on the use of biopolymers, and more particularly chitosan, for supporting catalytic precious metals (18–25). There are many reasons for this increasing interest in using chitosan as a catalytic support. This biopolymer has historically been used for biocatalysis (immobilizing enzymes at the surface of chitosan particles or in the core of chitosan gel beads) (26, 27). Extending the application to chemical catalysis is a logical continuation of this initial development. There are other reasons as well, such as the high affinity of this amino-polysaccharide for metal ions (28, 29), especially for precious metal anions (30). Chitosan is very efficient at sorbing metal cations through chelation in near-neutral solutions (28); however, due to its acid-base properties (intrinsic pK_a close to 6.5) in acidic solutions, the protonation of amine groups gives the polymer beneficial anion-exchange properties (31, 32). Chloro-complexes of platinum and palladium are readily adsorbed on protonated chitosan in acid media through electrostatic attraction (30). However, the solubility of chitosan in acidic solutions requires a pretreatment step consisting of the cross-linking of polymer

chains to chemically stabilize them, using, for example, glutaraldehyde as the cross-linking agent (30–32).

Preliminary experiments were performed on chromate reduction in order to optimize catalyst preparation (33). Research continued with the investigation of reductive chlorophenol dehalogenation using chitosan in the conditioning of flakes and beads (31). Interestingly, the dehalogenation of chlorophenol led to the production of cyclohexanol/cyclohexanone, indicating that a complementary dearomatization step took place during the transformation. The present work focuses on the study of nitrophenol degradation using chitosan-based materials. Several methods of conditioning the polymer will be tested, making use of another advantage of chitosan. Indeed, this material is very versatile and can be readily modified not only chemically (by grafting new functional groups) but also physically (via preparation of gel beads, membranes, fibers, and hollow fibers). Previous research has shown that diffusion limitations make a significant contribution to kinetic control (24). Actually, it seems that the catalytic reaction takes place exclusively at the surface (or in the outer layers) of the catalytic particles (25). In order to illustrate these limitations, a brief overview of results obtained in nitrophenol degradation will be presented using Pd supported on chitosan flakes. There are two possibilities to overcome these limitations: (a) using thin films immobilized on inert supports with a high specific surface area (20) and (b) developing a new conditioning method for the chitosan. This second option was selected for this part of the work, and hollow fibers were prepared and tested for nitrophenol degradation. In this case, in contrast with the batch test used with flakes, the system was operated by flowing the solution to be treated through the lumen of the fiber while the reducing agent was circulated outside the fiber (reagent compartment). In the case of flaked particles, nitrophenol hydrogenation was performed in the presence of sodium formate (as the hydrogen donor), leading to the formation of aminophenol and, depending on experimental conditions (lack of reducing agent), to some oxidized subproducts. In the case of hollow chitosan fibers, two hydrogenation systems were tested: (a) sodium formate in the reagent compartment recirculated with a pH control and (b) hydrogen gas maintained at the required pressure in the reagent compartment (Fig. 1).

MATERIAL AND METHODS

Materials

Previously characterized chitosan was supplied by Aber Technologies (Plouvien, France). The degree of deacetylation was 87% as measured by Fourier transform infrared (FTIR); the molecular weight (MW_n) was

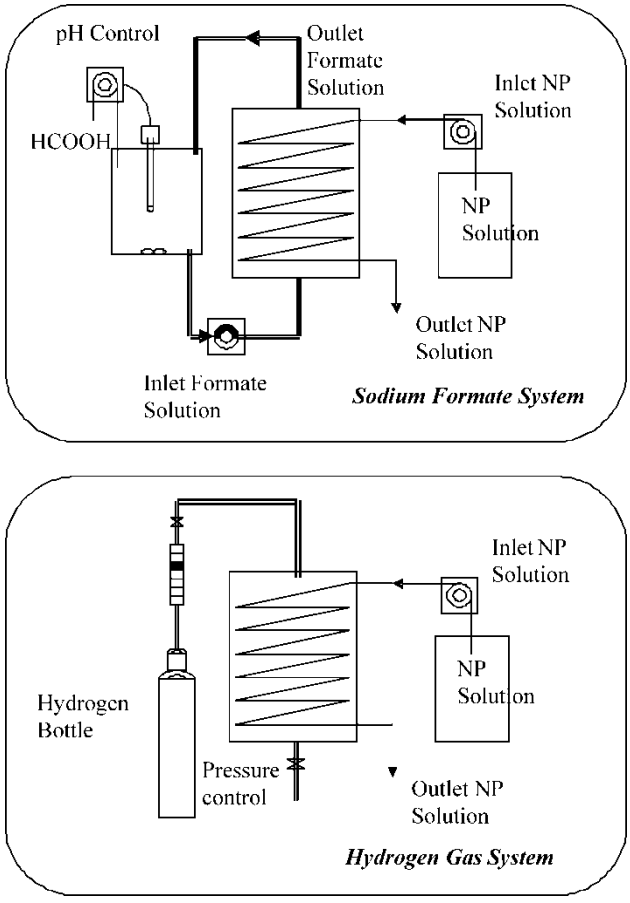

Figure 1. Experimental setup for 3-NP hydrogenation using catalytic hollow fibers.

125,000 g mol^{-1}, determined via size-exclusion chromatography coupled with a light-scattering photometer and a refractometer (Dawn F. Wyatt Technology, USA). Chitosan was ground and sieved to separate it into samples of different particle sizes: $0 < G0 < 63\,\mu m < G1 < 125\,\mu m < G2 < 250\,\mu m < G3 < 500\,\mu m < G4 < 710\,\mu m$. Another sample (G0b) was prepared by grinding the G4 fraction of the catalyst (after metal impregnation and reduction) and sieving the final powder to select the 0–63-μm-size fraction. For the preparation of hollow chitosan fibers, a chitosan of squid origin was kindly donated by Mahtani Chitosan Pvt (India). This sample was characterized using the same methods. The degree of deacetylation was 85%, and the value for MW_n was 365,000 g mol^{-1}. Nitrophenol (3-NP) was purchased from Fluka (Switzerland) as an analytical grade product, and

$PdCl_2$ was purchased from Acros (USA). Other reagents (acids, zinc, HCOONa) were supplied by Carlo Erba (Italy) as analytical-grade products.

The preparation of hollow chitosan fibers has been described in a previous paper (34). The main steps in the manufacturing process are described next. Hollow fibers of chitosan were produced by casting a viscous chitosan solution (in acetic acid) into a coagulating bath using a procedure derived from Kaminski et al. (35) and Agboh and Qin (36). The chitosan was dissolved in an acetic acid solution, with a small excess of organic acid compared with the molar concentration of amine groups. Typically, the solution was 4% w/w in both chitosan and acetic acid. The solution was then filtered to remove undissolved or colloidal particles. The solution was debubbled (under vacuum), and the polymeric solution was then dropped into a tank maintained at constant air pressure (4 bars). The solution was then extruded into an alkaline coagulating bath. After external coagulation, the lumen of the fiber was emptied by withdrawing noncoagulated chitosan by means of airflow followed by water flow. The final fiber was obtained by treatment with alkali. Finally, fibers were dried at room temperature. The external diameter of the fiber was 1.1 ± 0.1 mm, and the thickness of the fiber wall was 0.1 ± 0.015 mm. Figure 2 shows a scanning electron micrograph (SEM) of the fiber after air drying.

Sorbent Pretreatment

Since chitosan is soluble in hydrochloric acid, it cannot be used as supplied and a cross-linking treatment is required. Chitosan was cross-linked with glutaraldehyde by contact of chitosan with glutaraldehyde solution (10%, w/w).

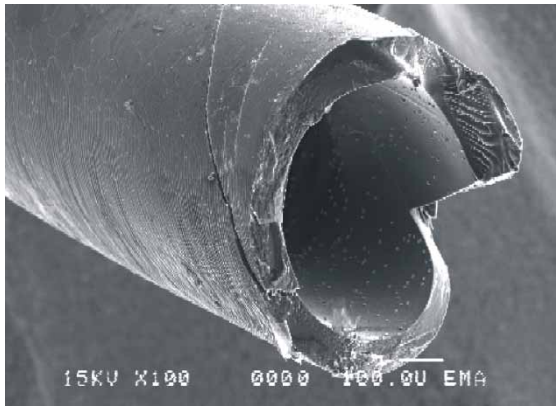

Figure 2. SEM photograph of hollow chitosan fiber.

The volume of glutaraldehyde solution and the mass of chitosan were set to reach a 1:1 molar ratio between the amine groups of the polymer and the aldehyde functions of the cross-linking agent. Finally, the particles were abundantly rinsed to remove traces of unreacted glutaraldehyde and dried at 60°C. However, this reaction has a serious drawback; in the case of hollow-fiber preparation makes the fiber very brittle. Therefore, it was preferable to condition the fiber in a sodium sulfate solution ($1\,g\,L^{-1}$) overnight at pH close to neutrality (pH 6.5–7.5) prior to metal sorption.

Palladium Sorption

The sorbent (1 g) was mixed for 24 h with a palladium solution (2 L) at a concentration of 200 mg Pd L^{-1} at pH 2. The solutions were then filtered, and the residual concentration of palladium in the solution was measured using inductively coupled plasma – atomic emission spectrometry (ICP-AES, Jobin-Yvon JY 2000, Longjumeau, France). The sorption capacity (amount of palladium adsorbed on the sorbent, q, mg Pd g^{-1}) was obtained by the mass balance equation.

Procedures for Palladium Reduction

The reduction treatment consisted of bringing the loaded sorbent (200 mg) into contact with 100 mL of sulfuric acid solution (1% w/w) with 300 mg of zinc (provided as a fine powder). By taking into account the change in the weight of the solid during the sorption and reduction steps, it was possible to calculate the amount of palladium contained in the final product. The palladium content was close to $105\,mg\,Pd\,g^{-1}$. A digestion/mineralization procedure (contact of the catalyst with a hydrochloric acid and hydrogen peroxide mixture) was used to disrupt the polymer and dissolve the metal. ICP analysis confirmed the actual palladium content: $102\,mg\,Pd\,g^{-1}$ catalyst. Other samples were prepared with higher concentrations of palladium in the loading bath and with different particle sizes. The same procedure was used to determine the palladium content: 153, 144, 132, and $124\,mg\,Pd\,g^{-1}$, for G1, G2, G3, and G4, respectively.

A sample of the fiber was digested with a mixture of sulfuric acid (1 mL, 36 M) and hydrogen peroxide (0.5 mL, 10 M) to completely degrade the support and dissolve palladium to analyze metal content using ICP-AES. The palladium content in the fiber was determined to be 4.2% (w/w); this value was consistent with that obtained using the mass balance equation for the sorption procedure. The water content of the fiber (after rehydration) was 62%. The length of the fibers (hydrated) used for these experiments was set at 1.3 m; the internal diameter was $500\,\mu m \pm 15\,\mu m$. The internal

volume of the fibers was 273 μL ± 5 μL. The amount of palladium present on the fiber was 4.09 mg (for a total fiber mass of approximately 97.5 mg).

Characterization of the Catalysts

Transmission electron microscopy (TEM) was used to measure the size of Pd nodules or crystals on the chitosan flakes. Catalyst particles were incorporated in a liquid resin. After cross-linking of the resin, thin slices of resins (60 μm) were cut using a microtome. TEM observations showed that the size of metal crystals was close to 4–5 nm. This is a critical parameter for catalytic activity. The smaller the size of catalyst nodules, the greater is the activity (37). The particles were highly dispersed in the material, though a slight gradient was observed between the center and the periphery of the particles. Some aggregates were also observed—the agglomeration of small nodules led to the formation of large palladium particles (around 30 nm). X-ray photoelectron spectroscopy (XPS) analysis was also performed in order to determine the oxidation state of palladium on the catalyst. It was shown that only 50 to 60% of palladium was reduced from Pd(II) to Pd(0).

Procedure for Nitrophenol Degradation

Nitrophenol was degraded by contacting 50 mL of a nitrophenol solution, containing the organic compound at a concentration of 50 mg L^{-1} (0.36 mM), with sodium formate at a concentration of 25 mM and 10 mg of catalyst (flakes). Unless otherwise specified, nitrophenol was used as 3-NP. The pH was initially controlled at pH 3 (unless otherwise specified) using a molar sulfuric acid solution. Samples were collected at selected contact times and filtered. After the sample (1-mL volume) had been acidified with 20 μL of sulfuric acid solution (5% w/w), the filtrates were analyzed using a UV spectrophotometer (Varian 2050) and by measuring the absorbance of the solutions at 332 nm.

With the hollow-fiber system, the ends of the catalytic fiber were connected to thin nozzles fed with a solution pumped from the nitrophenol solution reservoir, and the fibers were arranged in a closed tube connected to a tank of sodium formate or a bottle of hydrogen gas (see Fig. 1). In the case where sodium formate was used as the hydrogen donor, the formate solution was recycled and its pH was controlled at pH 4 using formic acid. Samples were collected at the outlet of the fiber, and the nitrophenol concentration was determined every 15 min. The concentration of nitrophenol in the sodium formate solution was also measured at the end of the experiment to check the transfer of the phenolic compound through the fiber. Mass balance on nitrophenol was used to evaluate the mean conversion yield,

taking into account the concentration of phenolic compound in both the formate solution and the treated effluent, as well as the volume of solution actually treated. The degradation efficiency was obtained by a mass balance equation (as the ratio of degraded nitrophenol to the initial concentration of the phenolic compound), and the catalytic activity (mmol NP h^{-1} g^{-1} Pd) was obtained from the degradation efficiency (DE), the initial concentration (C_0, mg L^{-1} or mmol L^{-1}), the volume of solution passed through the fiber (V, L), and the amount of palladium (m_{Pd}) present on the fiber (i.e., 4.09 mg):

$$CA = \frac{DE^{*}Co^{*}V}{m_{Pd}}$$

In the case where hydrogen gas was used as the hydrogen donor, the same experimental procedure was used. However, in this case, the residual concentration of nitrophenol was measured only at the outlet of the fiber. Nitrophenol degradation efficiency was obtained by comparing the outlet and inlet concentrations, and the catalytic activity was obtained using a mass balance similar to that used for the calculations in the sodium formate system.

Test experiments were performed to check the actual influence of catalyst and hydrogen donor. Fibers without palladium and catalytic fibers without hydrogen donor were tested to verify that sorption on the materials was negligible compared with the conversion efficiency of the catalytic systems.

RESULTS AND DISCUSSION

Preliminary Evaluation of the Experimental pH Range for Catalytic Conversion of Nitrophenol

Several experiments were performed at different pHs of nitrophenol solutions (in the range 2.2–5) to determine the optimum pH range for nitrophenol degradation. Degradation efficiency showed a marked preference for the medium-acid pH range. Actually, both kinetic rates and degradation efficiency were optimum at pH close to 3–4 (25). For the catalyst in the form of flakes, experiments were performed at pH 3. The glutaraldehyde cross-linking prevented degradation of the polymer in acidic solutions. In the case of hollow fibers, as explained previously, treatment of chitosan with glutaraldehyde is not possible since it makes the fibers very brittle. Additional linkages are created between polymer chains, resulting in loss of flexibility. The fibers were therefore conditioned in sulfate solutions. Though this pretreatment seemed sufficient for the sorption of palladium in HCl solutions,

it was decided to limit the potential hazards of fiber degradation by working at a higher pH (∼pH 4).

Catalyst Flakes

Conversion of nitrophenol into aminophenol

The reductive hydrogenation of 3-NP by sodium formate (catalyzed by Pd supported on chitosan flakes) was studied by UV spectrometry over 24 h of contact time. Two phases in the process were identified. During the first 1–2 h, nitrophenol was converted into aminophenol, as shown by UV spectrometry (Fig. 3, top); sodium formate was degraded into carbon dioxide

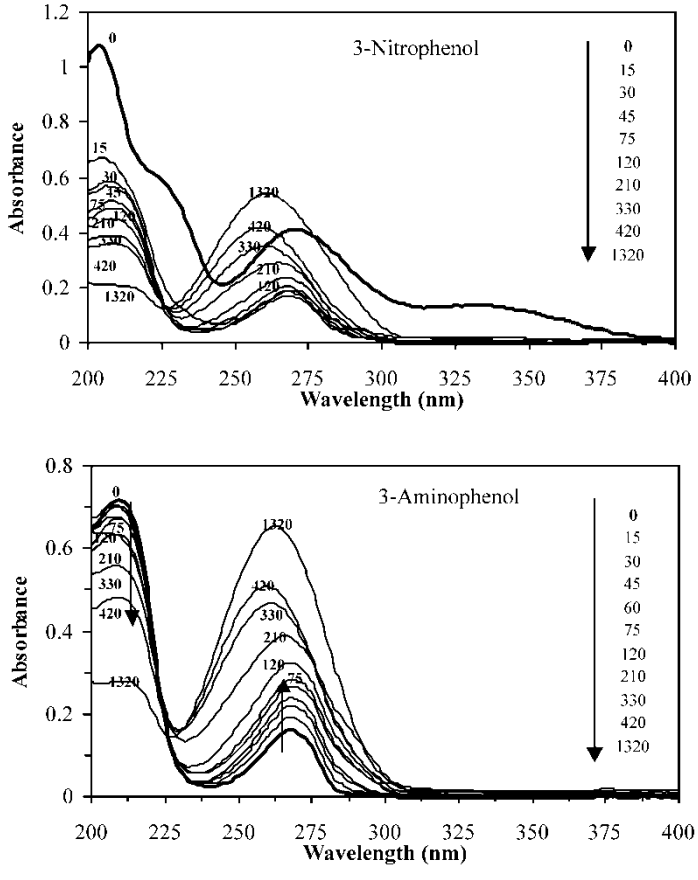

Figure 3. UV-visible spectra of the 3-NP and 3-AP during catalytic conversion with catalytic flaked chitosan particles as a function of time.

and the pH increased. Simultaneously, hydrogen was transferred and served to hydrogenate nitrate functions into amine functions. However, at long contact time (above 120–150 min), the peak at a wavelength of 268 nm, which is representative of aminophenol, was progressively shifted toward a slightly (but significantly) lower wavelength (~260 nm). Simultaneously, the intensity of the band increased. In order to verify the mechanism, a similar experiment was performed directly on 3-aminophenol (3-AP) (Fig. 3, bottom). The same results were obtained. During the first 2 h, the intensity of the peak at 268 nm increased. However, above 2.5 h of reaction time, there was a shift in the wavelength of the maximum peak to 260 nm, which occurred simultaneously with the increase in intensity. In the case of both nitro- and aminophenol, the peaks at 205 nm and 210 nm (respectively) continuously decreased. Additionally, in the case of nitrophenol degradation, the peaks representative of the nitrate function at 225–230 nm and 331 nm rapidly disappeared. A similar experiment was performed with phenol (not shown). However, in this case the phenol peak at 266 − 268 nm was not affected even after 24 h of reaction. The only changes in the spectra were recorded in the 204–206-nm wavelength range (certainly due to formate degradation). From these experiments, it appeared that the hydrogenation of nitrate occurred very rapidly (under the selected experimental conditions) and that (at long contact time) a secondary reaction occurred, contributing to the oxidation of aminophenol by the air atmosphere. These secondary reactions occurred directly at the aminophenol compound stage since phenol was not degraded under similar conditions. Due to the complexity of nitrophenol transformations, it was decided to track the disappearance of nitrophenol rather than the formation of other products.

Influence of diffusion limitations on conversion efficiency and catalytic activity for flaked particles

Though scanning electron microscopy–energy-dispersive X-ray (SEM-EDAX) analysis showed that the sorption of precious metals occurred in the whole mass of the sorbent and not exclusively at the external layers of the particles, diffusion limitations (especially resistance to intraparticle diffusion) have a powerful influence on kinetics for the diffusion of polynuclear species, especially in the case of the cross-linked material. We can therefore assume that palladium is almost homogeneously distributed in the particle. This was confirmed by TEM analysis. It is thus important to determine whether all the palladium nodules, even those located at the center of the particle, contribute to the reaction. For this reason some experiments were performed using chitosan flakes of different sizes (Fig. 4). The size of catalyst particles strongly influenced the time required to completely convert nitrophenol. While G3 and G4 particle sizes had quite similar kinetic curves, the differences were significantly more marked for the G0 to

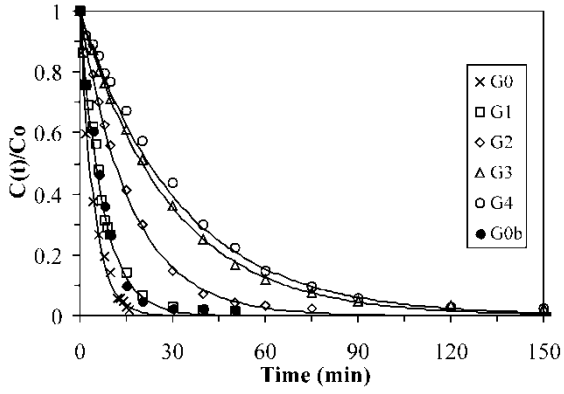

Figure 4. Influence of the particle size of catalytic flaked chitosan particles on 3-NP conversion kinetics (formate: 25 mM; NP: 50 mg L^{-1}; catalyst dosage: 200 mg L^{-1}).

G3 size fractions. Note that because of the flake shape of catalyst particles, for large particle sizes the sieving dimension is not really representative of the diffusion thickness. The differences may be explained by several factors: (a) heterogeneities in the distribution of Pd over the particle, (b) heterogeneous reduction of Pd [Pd(0) being the only active oxidation state], and (c) diffusion limitations. Though a difference has been observed on TEM in the distribution of Pd over the particle (a small gradient in the distribution of Pd nodules was noticed), this difference does not seem to be sufficient to explain such large differences in the kinetic profiles. The reduction procedure for Pd may introduce disparities in the reduction of Pd through the particle. Indeed, XPS analysis showed that the selected procedure did not reduce the total quantity of palladium at the surface of the catalyst (about 60%). To check the effect of heterogeneities on the catalytic behavior, a complementary experiment was performed using the largest particles (i.e., the G4 particles) following a grinding step (after metal sorption on large chitosan flakes and metal reduction in situ); the sample was ground to a particle size corresponding to the G0 size fraction. This experiment, performed under the same experimental conditions, is referred to as G0b in Fig. 4. Obviously, the grinding of the large particles enabled catalytic performance to be restored, and the kinetic curve was located between curves G0 and G1. This indicates that though the effect of possible heterogeneities cannot be totally neglected, the main limiting effect is due to another reason: the effect of intraparticle diffusion resistance. It remains questionable whether the effect was (a) in the diffusion of the reagent and products or (b) in a reaction that was limited exclusively to the external part of the particle. Complementary experiments (not shown) were performed with catalysts loaded with different amounts of palladium.

It appeared that increasing the loading of the catalyst slightly improved kinetics (but not proportionally to metal quantity) but resulted in a decrease in the catalytic activity coefficient (CAC, reported as the amount of nitrophenol degraded by time unit and Pd mass unit). The best efficiency in the use of Pd was obtained at lower Pd-loading. Similar experiments with different dosages of catalyst showed that the CAC decreased when the amount of catalyst was increased: a better use of the metal was achieved via small catalyst dosages. Intraparticle diffusion resistance certainly contributes to the limitation of kinetic rates, and most of the reaction occurs at the external surface of the catalyst particle.

Another possible limiting step is external diffusion. Its influence is usually measured through the influence of agitation. Figure 5 shows degradation curves for agitation velocities between 100 and 750 rps. Though the kinetic profile became slightly more favorable with increasing agitation velocity, this parameter actually had a limited effect on degradation kinetics. Resistance to film diffusion cannot be considered a controlling parameter in the degradation process.

Minimum required molar ratio of nitrophenol to formate required for complete conversion of nitrophenol

Another important parameter in the design of the catalytic system is the definition of reducing conditions, and more specifically the concentrations of reducing agent (i.e., sodium formate) required for the complete conversion of nitrophenol. Figure 6 shows the kinetic profiles for nirophenol degradation (at the concentration 50 mg L^{-1}) with increasing concentrations of sodium

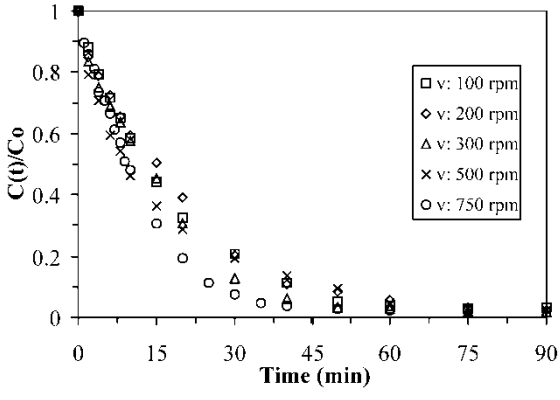

Figure 5. Influence of agitation velocity on 3-NP conversion kinetics with catalytic flaked chitosan particles (formate: 25 mM; NP: 50 mg L^{-1}; catalyst dosage: 200 mg L^{-1}).

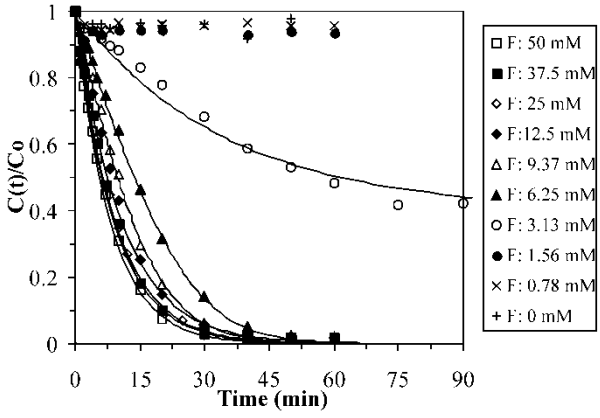

Figure 6. Influence of formate concentration on 3-NP conversion kinetics with catalytic flaked chitosan particles (NP: 50 mg L^{-1}; catalyst dosage: 200 mg L^{-1}).

formate. Below a sodium formate concentration of approximately 2 mM, nitrophenol degradation was negligible. In the range 2–6 mM, formate concentration was not high enough to completely convert nitrophenol into aminophenol. However, above 6 mM, conversion of the substrate was complete. Above 9 mM, increasing sodium formate concentration did not significantly improve degradation kinetics. The limiting molar ratio formate/3-NP for complete degradation of the substrate was found to be close to 10–15. Similar trends were obtained by varying nitrophenol concentration for a given formate concentration (not shown). This limiting ratio may be decreased by increasing the reaction temperature.

Influence of temperature on nitrophenol conversion

Figure 7 shows the kinetic profiles for nitrophenol degradation at different temperatures. Obviously, the temperature had a significant effect on reaction kinetics. The reaction is endothermic. However, the greatest difference was observed for the temperature increase from 10°C to 22°C, though the variations were also significant for other gaps: 22°C to 40°C and 40°C to 60°C. The activation energy was calculated for different catalyst dosages and varied between 17 and 26 kJ mol^{-1}. This is consistent with the activation energy (close to 21 kJ mol^{-1}) found by Vincent et al. (24) for chlorophenol dehalogenation with the same catalyst. It is interesting to observe that this value is comparable to the activation energy calculated from data obtained by Gallezot et al. (36) for formic acid oxidation by a platinum catalyst immobilized on activated carbon ($\sim$26.4 kJ mol^{-1}). It is about three times higher than the activation energy found by Lea and Adesina (37) for the oxidative degradation

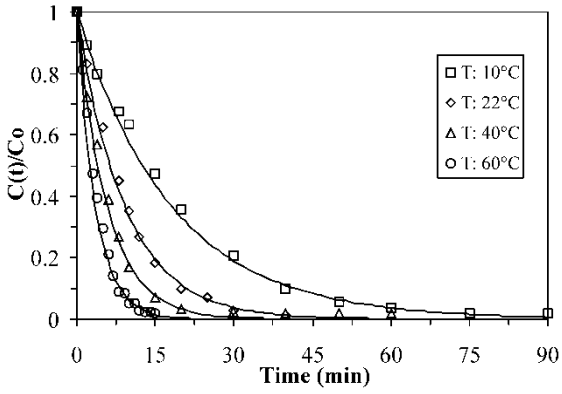

Figure 7. Influence of temperature on 3-NP conversion kinetics with catalytic flaked chitosan particles (formate: 25 mM; NP: 50 mg L^{-1}; catalyst dosage: 200 mg L^{-1}).

of 4-nitrophenol using a photocatalytic process (about 8 kJ mol^{-1}). Felis et al. (38) found higher activation energy values for the hydrodechlorination of chlorophenol and the dearomatization of the intermediary products, using Ru/C catalysts: about 45 kJ mol^{-1} and 33 kJ mol^{-1}, respectively. Since the objective is to develop an energy-efficient process, the temperature was maintained in the 20–22°C range for other experiments.

These experiments showed that most of the limitations on the degradation of nitrophenol using a chitosan-supported palladium catalyst can be attributed to a lack of reducing agent (a 10–15 molar excess is required for complete transformation of nitrophenol) and to limitations due to intraparticle diffusion. The reactions take place at the external surface of the catalyst. As a consequence, the use of palladium is not optimized (internal metal sites do not contribute). In order to achieve a better use of this precious metal in the manufacturing and use of the catalyst, it is better to use chitosan in a thin-layer conditioned form. Two processes may be proposed: (a) depositing chitosan at the surface of an inert and very porous (high-specific-surface-area) support or (b) using thin membranes of chitosan. This second option was selected, using an original form of chitosan material (i.e., hollow fibers).

Hollow Fibers

Influence of hydrogen donor concentration or pressure on conversion efficiency

As pointed out in the case of the flaked material, a key parameter was the concentration of the hydrogen donor (sodium formate). The first step in the study

of the hollow-fiber system was therefore to measure the effect of this parameter on treatment efficiency. Since two hollow-fiber systems were operated, depending on the type of hydrogen donor (i.e., sodium formate and hydrogen gas), the pressure of hydrogen gas was also varied. Results are given in Fig. 8. Solid lines on the figure should be considered to be

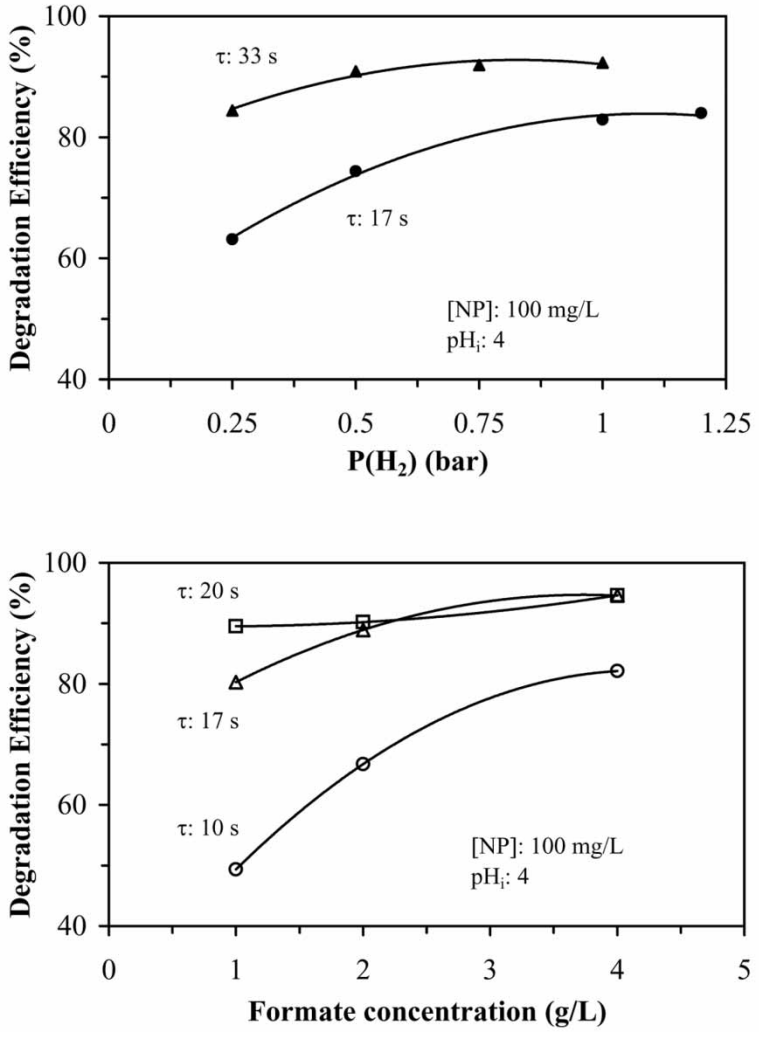

Figure 8. Influence of concentration (or pressure) of hydrogen donor (sodium formate, top; hydrogen gas, bottom) on 3-NP conversion efficiency (after 1 h of operating time) with catalytic hollow chitosan fiber.

indicative of the trend followed by degradation curves; actually, the degradation efficiency tended to level off at high hydrogen donor concentration or pressure. The experiments were performed at different flow rates of the solution (circulating in the lumen of the fiber). Therefore, curves have been plotted in function of sodium formate concentration (or hydrogen pressure) for different residence times (τ) in the fiber. Whatever the reducing system, increasing the concentration (or pressure) increased the efficiency of degradation. However, the enhancement of the conversion was strictly controlled by the residence time. At short contact time (i.e., τ: 10 sec for sodium formate system), conversion increased from 50 to 90% when sodium formate concentration was increased from $1\,g\,L^{-1}$ to $4\,g\,L^{-1}$. On the other hand, for the same variation in concentration, the degradation efficiency was hardly changed (from 90 to 92%) by increasing residence time to 20 sec. Increasing the concentration of sodium formate tended to level off the influence of residence time. This cross-effect of residence time and sodium formate concentration indicates that the efficiency of the system is controlled by the availability of sodium formate, related to its diffusion properties through the membranes. This appears to be the limiting step. Similar trends were observed in the case of hydrogen gas system. Increasing hydrogen pressure increased the efficiency of the conversion process, especially at short residence time (i.e., τ: 17 sec); increasing the residence time to 33 sec significantly decreased the impact of hydrogen pressure on conversion efficiency. Generally sodium formate proved more efficient than hydrogen gas for reducing nitrophenol to aminophenol: for the same residence time, depending on the concentration of hydrogen donor, the sodium formate system reached a conversion efficiency 10 to 15% higher than the levels reached with the hydrogen gas system. To obtain the same levels of degradation efficiency (about 90%), it was necessary to significantly increase residence time to 33 sec as compared with 20 sec in the case of the sodium formate system. However, it is important to observe that the hydrogen gas system proved efficient, even for low hydrogen pressure (0.5 bar). The system sounds promising since on-demand delivery of hydrogen enabled gas consumption to be reduced. The gas is maintained at constant pressure in the closed compartment, and its consumption is controlled by the diffusion of the gas through the membrane. Another advantage of the hydrogen gas system is the reduced impact of subproducts on the environment of the process. The diffusion of nitrophenol through the membrane into the sodium formate compartment contributed to the contamination of this solution, though the transferred fraction was quite low (less than 5% of the amount treated). However, the mean degradation efficiency calculated from the mass balance equation for a 1 h reaction time is not the only parameter to be taken into account in evaluating the efficiency of the process. Samples were regularly collected (every 15 min) to check the stability of the degradation and detect limiting criteria. Figure 9 shows that with a formate

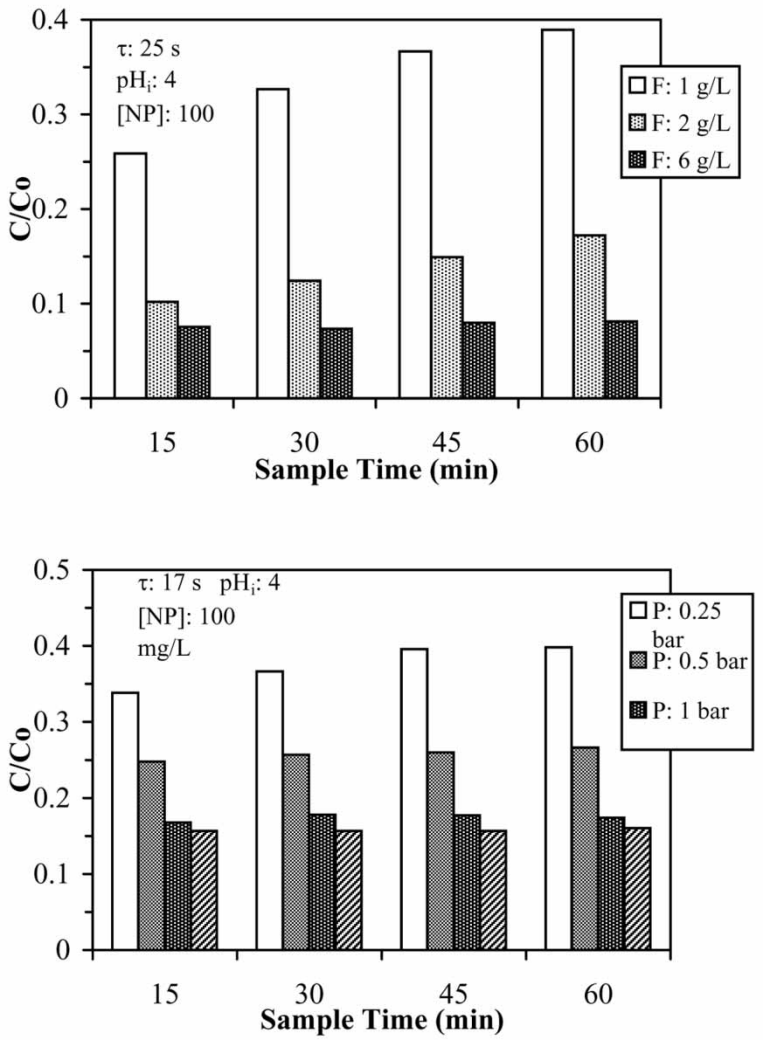

Figure 9. Influence of concentration (or pressure) of hydrogen donor (sodium formate, top; hydrogen gas, bottom) on 3-NP relative concentration at the outlet of the catalytic hollow chitosan fiber at given contact times.

concentration equal to or below $2\,g\,L^{-1}$, the efficiency progressively decreased under the selected experimental conditions (concentration and residence time), while with hydrogen gas the limiting pressure for efficient and stable degradation corresponded to a value of 0.5 bar. Though the degradation efficiency was higher with formate as the hydrogen donor, it is

important to observe that using hydrogen gas increased the stability of the conversion over time.

Influence of residence time on conversion efficiency

The strong effect of residence time (τ) on the catalytic reaction in the continuous mode was clearly identified in the preceding section. It appeared to be necessary to continue the evaluation of this experimental parameter by varying residence time for given concentrations of sodium formate (1, 2, and 4 $g\,L^{-1}$) and given pressures of hydrogen gas (i.e., 0.5 and 1 bar). Results are summarized in Fig. 10. As expected, the conversion efficiency increased with increasing residence time, for both sodium formate and hydrogen gas (whatever the concentration or pressure). However, above a certain residence time, the curves tended to level off. The specific residence time depended on the hydrogen donor and the concentration or pressure. Although 20 sec was sufficient in the case of sodium formate (1 $g\,L^{-1}$) and hydrogen gas at a pressure of 1 bar, it was necessary to increase the residence time to 30–35 sec to reach the same conversion efficiency ($\sim$95 %) when hydrogen pressure was reduced to 0.5 bar. The curve representing sodium formate at a concentration of 1 $g\,L^{-1}$ becomes superimposed over the one obtained with hydrogen gas at a pressure of 1 bar. Under these experimental conditions the performances are equivalent.

Considering the stability of the conversion over time, Fig. 11 shows that when formate concentration reached 4 $g\,L^{-1}$, the conversion remained stable throughout the 1 h processing time, while a significant decrease in conversion efficiency was observed above a residence time of 20 sec when the concentration of formate was 1 $g\,L^{-1}$. In the case of hydrogen at a pressure of

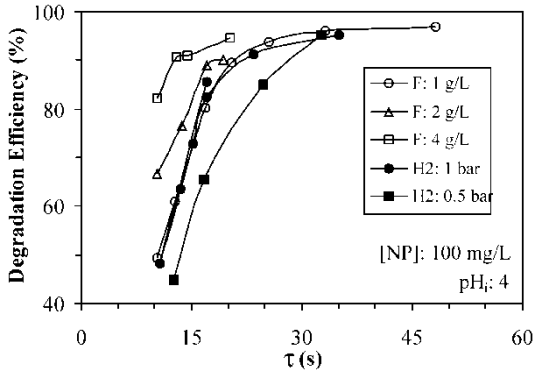

Figure 10. Influence of mean residence time of the solution in the fiber on 3-NP conversion efficiency (after 1 h of operating time) with catalytic hollow chitosan fiber.

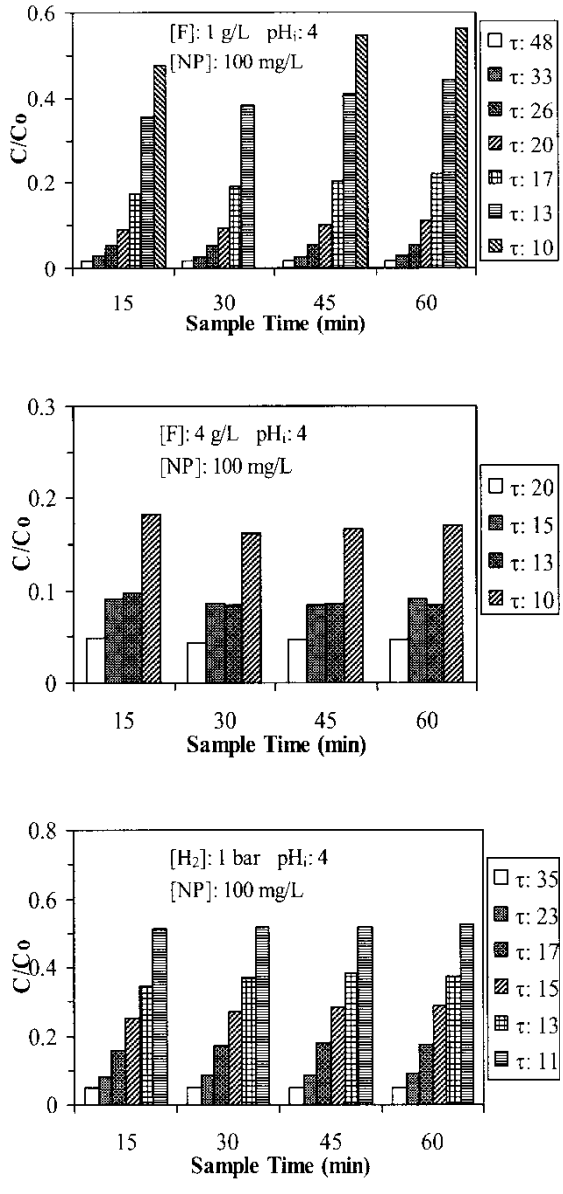

Figure 11. Influence of mean residence time of the solution in the fiber on 3-NP relative concentration at the outlet of the fiber at given contact times for different hydrogen donors: sodium formate (at two different concentrations), top and middle panel; hydrogen gas, bottom panel.

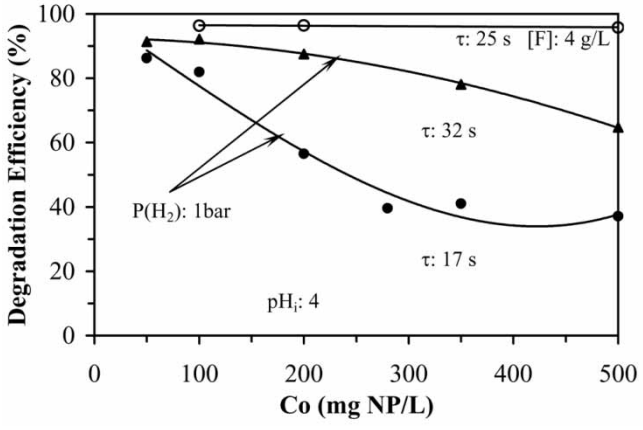

Figure 12. Influence of substrate (3-NP) concentration on 3-NP conversion efficiency (after 1 h of operating time) with catalytic hollow chitosan fiber using sodium formate and hydrogen gas as hydrogen donor.

1 bar, the conversion remained stable over 1 h of operation without any significant change in the efficiency.

Influence of nitrophenol concentration on conversion efficiency

The concentration of nitrophenol at the inlet of the fiber is also an important parameter in the evaluation of the process. Figure 12 shows the data obtained with both the sodium formate and the hydrogen gas system (for different residence times in the latter case). At a formate concentration of $4\,g\,L^{-1}$, the concentration of nitrophenol did not change the conversion efficiency (around 97%) in the concentration range investigated ($\sim 100-500\,mg\,NP\,L^{-1}$). In the case of hydrogen gas, the behavior is significantly different. With a hydrogen pressure of 1 bar, the conversion progressively decreased from 92% to 65% at long residence times ($\sim 32\,sec$), while the decrease was significantly greater at short residence time ($\sim 17\,sec$), from 88% to 40%.

The stability in the conversion of nitrophenol to aminophenol was slightly affected by substrate concentration: a slight decrease in efficiency was observed at the highest concentrations for both the sodium formate and the hydrogen system (Fig. 13). However, the variation in the relative concentration at the outlet of the fiber was remarkably low with formate as the hydrogen donor at this concentration ($\sim 4\,g\,L^{-1}$).

The catalytic hollow fibers may be operated using two different configurations with different hydrogen donors. Though using sodium formate as the hydrogen donor substantially increased nitrophenol conversion compared with the hydrogen gas system, it was necessary to use high formate

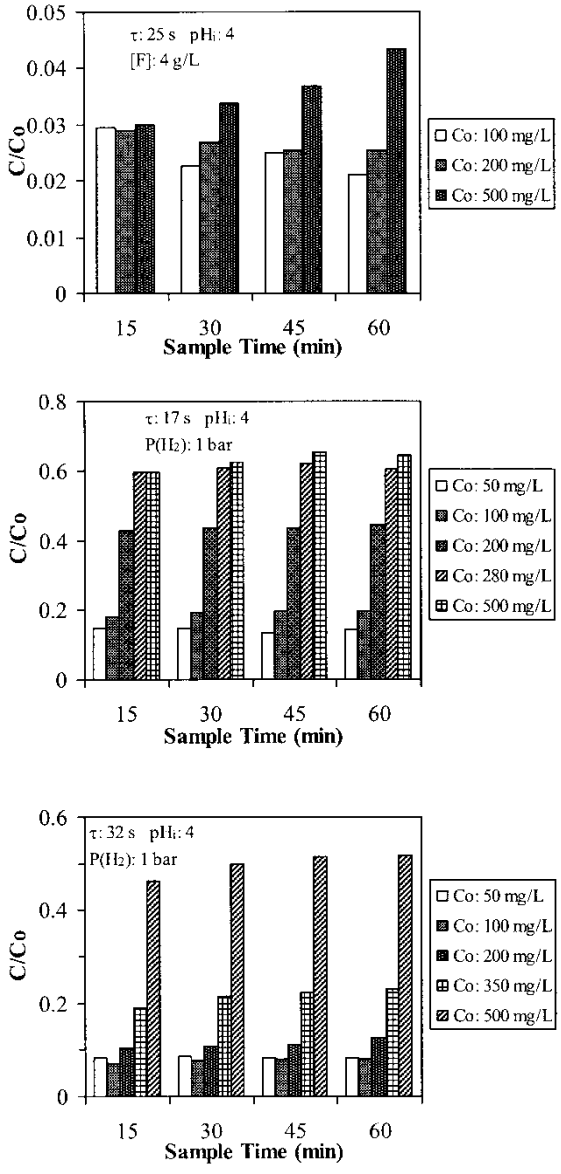

Figure 13. Influence of substrate (3-NP) concentration on 3-NP relative concentration at the outlet of the fiber at given contact times for different hydrogen donors: sodium formate, top panel; hydrogen gas (at two different mean residence times), middle and bottom panels.

concentration ($\sim 4\,g\,L^{-1}$) to maintain conversion efficiency at a stable level for a 1 h operating time. The system using hydrogen gas, though less efficient in terms of conversion efficiency, required only 0.5–1-bar gas pressure to maintain a stable catalytic activity.

CONCLUSIONS

Chitosan was used effectively for the preparation of a supported palladium catalyst. The high efficiency of chitosan for palladium sorption and the stability of the metal on loaded solid can explain the high efficiency of the catalyst (after in situ metal reduction) for conversion of nitrophenol into aminophenol (reaction used as a probe of catalytic hydrogenation). A strong limitation in the catalytic use of palladium was observed due to diffusion limitations; reaction was effectively limited to the external surface of the particle. In order to reduce diffusion limitations (and avoid using too small particles, which would make the system unsuitable for large-scale applications), hollow chitosan fibers were designed, loaded with palladium, and further chemically reduced. The new system was used with both hydrogen gas and sodium formate as hydrogen donors. The best performance was obtained using sodium formate, but using hydrogen as donor increased the stability of the catalytic activity (compared with low sodium formate concentration). Moreover, the hydrogen system avoided the production of secondary contaminated flows as had occurred with sodium formate (a small part of nitrophenol migrated through the fiber into the hydrogen donor compartment). Moreover, though the consumption of hydrogen was not measured, it seems that the system was highly efficient in terms of hydrogen use: low pressures were required (0.5–1 bar) and the compartment was only maintained under constant pressure. (It was not necessary to maintain a gas flow through the compartment.)

The system is currently being investigated for oxidation reactions, in this case using copper adsorbed on chitosan materials. This opens up a wide range of applications, taking advantage of the great versatility of the polymer (e.g., easy chemical modifications and great diversity in polymer conditioning and shape).

REFERENCES

1. Dutta, S., Basu, J.K., and Ghar, R.N. (2001) Studies on Adsorption of *p*-Nitrophenol on Charred Saw-Dust. *Sep. Purif. Technol.*, 21: 227–235.
2. Sismanoglu, T. and Pura, S. (2001) Adsorption of Aqueous Nitrophenols on Clinoptilolite. *Colloid Surf. A*, 180: 1–6.
3. Andreozzi, R., Caprio, V., Insola, A., Longo, G., and Tufano, V. (2000) Photocatalytic Oxidation of 4-Nitrophenol in Aqueous TiO_2 Slurries: An Experimental Validation of Literature Kinetic Models. *J. Chem. Tech. Biotechnol.*, 75: 131–136.

4. Goi, A. and Trapido, M. (2002) Hydrogen Peroxide Photolyse, Fenton Reagent and Photo-Fenton for the Degradation of Nitrophenols: A Comparative Study. *Chemosphere*, 46: 913–922.
5. Halligudi, S.B. and Khaire, S.S. (2001) Kinetics of Hydrogenation of 4-Chloro-2-Nitrophenol Catalyzed by Pt/Carbon Catalyst. *J. Chem. Techol. Biotechnol.*, 77 (1): 25–28.
6. Felis, V., De Bellefon, C., Fouilloux, P., and Schweich, D. (1999) Hydrodechlorination and Hydrodearomatisation of Monoaromatic Chlorophenols into Cyclohexanol on Ru/C Catalysts Applied to Water Depollution: Influence of the Basic Solvent and Kinetics of the Reactions. *Appl. Catal. B: Environ.*, 20 (2): 91–100.
7. Scirè, S., Minico, S., and Crisafulli, C. (2002) Selective Hydrogenation of Phenol to Cyclohexanone over Supported Pd and Pt-Ca Catalysts: An Investigation on the Influence of Different Supports and Pd Precursors. *Appl. Catal. A*, 235: 21–31.
8. Morales, J., Hutcheson, R., Noradoun, C., and Cheng, L.F. (2002) Hydrogenation of Phenol by the Pd/Mg and Pd/Fe Bimetallic Systems under Mild Reaction Conditions. *Ind. Eng. Chem. Res.*, 41 (13): 3071–3074.
9. Mahata, N. and Vishwanathan, V. (1997) Kinetics of Phenol Hydrogenation over Supported Palladium Catalyst. *J. Mol. Catal. A: Chem.*, 120: 267–270.
10. Rode, C.V., Vaidyn, M.J., and Chaudhari, R.V. (1999) Synthesis of *p*-Aminophenol by Catalytic Hydrogenation on Nitrobenzene. *Org. Process Res. Dev.*, 3 (6): 465–470.
11. Vaidya, M.J., Kulkarni, S.M., and Chaudhari, R.V. (2003) Synthesis of *p*-Aminophenol by Catalytic Hydrogenation of *p*-Nitrophenol. *Org. Process Res. Dev.*, 7 (2): 202–208.
12. Choudhary, V.R., Sane, M.G., and Tambe, S.S. (1998) Kinetics of Hydrogenation of *o*-Nitrophenol to *o*-Aminophenol on Pd/Carbon Catalysts in a Stirred Three-Phase Slurry Reactor. *Ind. Eng. Chem. Res.*, 37: 3879–3887.
13. Yuan, G. and Keane, M.A. (2003) Liquid Phase Catalytic Hydrodechlorination of 2,4 Dichlorophenol over Carbon Supported Palladium: An Evaluation of Transport Limitations. *Chem. Eng. Sci.*, 58: 257–267.
14. Shore, S.G., Ding, E., Park, C., and Keane, M.A. (2002) Vapor Phase Hydrogenation of Phenol over Silica Supported Pd and Pd-Yb Catalysts. *Catal. Commun.*, 3: 77–84.
15. Mahata, N., Raghavan, K.V., and Vishwanathan, V. (1999) Influence of Alkali Promotion on Phenol Hydrogenation Activity of Palladium/Alumina Catalysts. *Appl. Catal. A*, 182: 183–187.
16. Altava, B., Burguete, M.I., García-Verdugo, E., Luis, S.V., Vicent, M.J., and Mayoral, J.A. (2001) Supported Chiral Catalysts: The Role of the Polymeric Network. *React. Funct. Polym.*, 48: 125–135.
17. Drelinkiewicz, A. and Hasik, M. (2001) 2-Ethyl-9,10-Anthraquinone Hydrogenation over Pd/Polymers: Effect of Polymers-Pd(II) Chlorocomplexes Interactions. *J. Mol. Catal. A: Chem.*, 177 (1): 149–164.
18. Jin, J.-J., Chen, G.-C., Huang, M.-Y., and Jiang, Y.-Y. (1994) Catalytic Hydrogenation Behaviours of Palladium Complexes of Chitosan-Polyacrylic Acid and Chitosan Polymethacrylic Acid. *React. Polym.*, 23: 95–100.
19. Han, H.-S., Jiang, S.-N., Huang, M.-Y., and Jiang, Y.-Y. (1996) Catalytic Hydrogenation of Aromatic Nitro Compounds by Non-Noble Metal Complexes of Chitosan. *Polym. Adv. Technol.*, 7 (8): 704–706.

20. Yin, M.-Y., Yuan, G.-L., Wu, Y.-Q., Huang, M.-Y., and Jiang, Y.-Y. (1999) Asymmetric Hydrogenation of Ketones Catalyzed by a Silica-Supported Chitosan-Palladium Complex. *J. Mol. Catal. A: Chem.*, 147 (1–2): 93–98.
21. Quignard, F., Choplin, A., and Domard, A. (2000) Chitosan: A Natural Polymeric Support of Catalysis for the Synthesis of Fine Chemicals. *Langmuir*, 16: 9106–9109.
22. Guo, C.-C., Huang, G., Zhang, X.-B., and Guo, D.-C. (2003) Catalysis of Chitosan-Supported Iron Tetraphenylporphyrin for Aerobic Oxidation of Cyclohexane in Absence of Reductants and Solvents. *Appl. Catal. A: Gen.*, 247: 261–267.
23. Kucherov, A.V., Kramereva, N.V., Finashina, E.D., Koklin, A.E., and Kustov, L.M. (2003) Heterogenized Redox Catalysts on the Basis of the Chitosan Matrix 1. Copper Complexes. *J. Mol. Catal. A: Gen.*, 198: 377–389.
24. Vincent, T., Spinelli, S., and Guibal, E. (2003) Chitosan-Supported Palladium Catalyst. II. Chlorophenol Dehalogenation. *Ind. Eng. Chem. Res.*, 42 (24): 5968–5976.
25. Vincent, T. and Guibal, E. (2003) Chitosan-Supported Palladium Catalyst. III. Influence of Experimental Parameters on Nitrophenol Degradation. *Langmuir*, 19 (20): 8475–8483.
26. Gonzalez Siso, M.I., Lang, E., Carreno-Gomez, B., Becerra, M., Otero Espinar, F., and Blanco Mendez, J. (1997) Enzyme Encapsulation on Chitosan Microbeads. *Process Biochem.*, 32 (3): 211–216.
27. Juang, R.-S., Wu, F.-C., and Tseng, R.-L. (2002) Use of Chemically Modified Chitosan Beads for Sorption and Enzyme Immobilization. *Adv. Environ. Res.*, 6: 171–177.
28. Bassi, R., Prasher, S.O., and Simpson, B.K. (2000) Removal of Selected Metal Ions from Aqueous Solutions Using Chitosan Flakes. *Sep. Sci. Technol.*, 35 (4): 547–560.
29. Inoue, K. (1998) Application of Chitosan in Separation and Purification of Metals. In *Recent Advances in Marine Biotechnology*; Fingerman, M., Nagabhushanam, R.Thompson, M.-F., Eds.; Oxford & IBH Publishing PVT. Ltd: New Delhi, 63–97.
30. Guibal, E., Ruiz, M., Vincent, T., Sastre, A., and Navarro Mendoza, R. (2001) Platinum and Palladium Sorption on Chitosan Derivatives. *Sep. Sci. Technol.*, 36 (5–6): 1017–1040.
31. Guibal, E., Milot, C., and Roussy, J. (2000) Influence of Hydrolysis Mechanisms on Molybdate Sorption Isotherms Using Chitosan. *Sep. Sci. Technol.*, 35 (7): 1021–1038.
32. Guzman, J., Saucedo, I., Revilla, J., Navarro, R., and Guibal, E. (2002) Vanadium(V) Interactions with Chitosan: Influence of Polymer Protonation and Metal Speciation. *Langmuir*, 18 (5): 1567–1573.
33. Vincent, T. and Guibal, E. (2002) Chitosan-Supported Palladium Catalyst. I. Synthesis Procedure. *Ind. Eng. Chem. Res.*, 41 (21): 5158–5164.
34. Vincent, T. and Guibal, E. (2001) Cr(VI) Extraction Using Aliquat 336 in Hollow Fiber Module Made of Chitosan. *Ind. Eng. Chem. Res.*, 40 (5): 1406–1411.
35. Mabbett, A.N., Yong, P., Baxter-Plant, V.S., Mikheenko, I.P., Farr, J.P.G., and Macaskie, L.E. (2001) Effective Reduction and Removal of Cr(VI) and Reductive Dehalogenation of Chlorophenol by Hybrid Bioinorganic Catalytic Processes. In *Biohydrometallurgy: Fundamentals, Technology and Sustainable Development*; Ciminelli, V.S.T., and Garcia, Jr.O., Ed.; Wiley: Amsterdam; 335–342.

36. Gallezot, P., Laurain, N., and Isnard, P. (1996) Catalytic Wet-Air Oxidation of Carboxylic Acids on Carbon-Supported Platinum Catalysts. *Appl. Catal. B: Environ.*, 9 (1–4): 11–17.
37. Lea, J. and Adesina, A.A. (2001) Oxidative Degradation of 4-Nitrophenol in UV-Illuminated Titania Suspension. *J. Chem. Techol. Biotechnol.*, 76: 803–810.
38. Felis, V., De Bellefon, C., Fouilloux, P., and Schweich, D. (1999) Hydrodechlorination and Hydrodearomatisation of Monoaromatic Chlorophenols into Cyclohexanol on Ru/C Catalysts Applied to Water Depollution: Influence of the Basic Solvent and Kinetics of the Reactions. *Appl. Catal. B: Environ.*, 20 (2): 91–100.